nature nanotechnology

ARTICLES

PUBLISHED ONLINE: 3 APRIL 2011 | DOI: 10.1038/NNANO.2011.41

Silica and titanium dioxide nanoparticles cause pregnancy complications in mice

Kohei Yamashita[1,2†], Yasuo Yoshioka[1,2,3†*], Kazuma Higashisaka[1,2], Kazuya Mimura[4], Yuki Morishita[1,2], Masatoshi Nozaki[4], Tokuyuki Yoshida[1,2], Toshinobu Ogura[1,2], Hiromi Nabeshi[1,2], Kazuya Nagano[2], Yasuhiro Abe[2], Haruhiko Kamada[2,3], Youko Monobe[5], Takayoshi Imazawa[5], Hisae Aoshima[6], Kiyoshi Shishido[7], Yuichi Kawai[8], Tadanori Mayumi[8], Shin-ichi Tsunoda[2,3,9], Norio Itoh[1], Tomoaki Yoshikawa[1,2], Itaru Yanagihara[4], Shigeru Saito[10] and Yasuo Tsutsumi[1,2,3*]

The increasing use of nanomaterials has raised concerns about their potential risks to human health. Recent studies have shown that nanoparticles can cross the placenta barrier in pregnant mice and cause neurotoxicity in their offspring, but a more detailed understanding of the effects of nanoparticles on pregnant animals remains elusive. Here, we show that silica and titanium dioxide nanoparticles with diameters of 70 nm and 35 nm, respectively, can cause pregnancy complications when injected intravenously into pregnant mice. The silica and titanium dioxide nanoparticles were found in the placenta, fetal liver and fetal brain. Mice treated with these nanoparticles had smaller uteri and smaller fetuses than untreated controls. Fullerene molecules and larger (300 and 1,000 nm) silica particles did not induce these complications. These detrimental effects are linked to structural and functional abnormalities in the placenta on the maternal side, and are abolished when the surfaces of the silica nanoparticles are modified with carboxyl and amine groups.

Nanomaterials such as nanosilica particles (nSPs), titanium dioxide nanoparticles (nano-TiO_2) and carbon nanotubes are already being applied in electronics[1], foods[2], cosmetics[3] and drug delivery[4]. nSPs are used as additives in cosmetics and foods because they are highly hydrophilic, easy to synthesize and their surfaces can be modified easily[5,6]. The increasing use of nanomaterials has raised concerns[7–9] because of recent reports showing that carbon nanotubes can induce mesothelioma-like lesions in mice, similar to those induced by asbestos[10,11]. We have also shown that nSPs can induce severe liver damage in mice and inflammatory responses *in vitro*[12,13].

Fetuses are known to be more sensitive to environmental toxins than adults[14–16], and it has been suggested that many chemical toxins in air, water and foods can induce pregnancy complications in humans[15,16]. An estimated 1 to 3% of women in the USA suffer recurrent miscarriages[17] and 7–15% of pregnancies are affected by poor fetal growth (a condition known as intrauterine growth restriction, IUGR)[18]. IUGR, which refers to a fetus with a weight below the 10th percentile for its gestational age, can cause fetal death and predisposes the child to a lifelong increased risk for cardiovascular disorders and renal disease[19,20]. Examining the potential risk of nanomaterials for causing miscarriage and IUGR is therefore essential.

Although some studies have shown transplacental transport of nanomaterials in pregnant animals and nanomaterial-induced neurotoxicity in their offspring[21–26], the effects of nanomaterials on pregnant animals have not yet been studied. Here, we investigated the biodistribution and fetotoxicity of various sizes of surface-modified nSPs, fullerene C_{60} and nano-TiO_2 in pregnant mice. Our results indicate that nSPs with diameters less than 100 nm and nano-TiO_2 with diameters of 35 nm induce resorption of embryos and fetal growth restriction. Furthermore, we found that modifying the surface of nSPs from –OH to –COOH or –NH_2 functional groups can prevent these pregnancy complications. These data include basic information regarding possible ways of creating safer nanomaterials.

Biodistribution of nanoparticles

Silica particles are well suited for studying the influence of nanomaterial size on biodistribution and various biological effects because they show much better dispersibility in aqueous solutions than most other nanomaterials[27]. We used silica particles with diameters of 70 nm (nSP70), 300 nm (nSP300) and 1,000 nm (mSP1000) to study the effect of size on biodistribution of the particles in pregnant mice. Two other common nanomaterials, nano-TiO_2 and fullerene, were also examined. All silica nanoparticles were confirmed by transmission electron microscopy (TEM) to be smooth-surfaced spheres (Supplementary Fig. S1a,b,c,g,h,i)[12,13]. The hydrodynamic diameters of nSP70, nSP300, mSP1000, nano-TiO_2 and fullerene were 65, 322, 1,140, 217 and 143 nm, respectively, with zeta

[1]Department of Toxicology and Safety Science, Graduate School of Pharmaceutical Sciences, Osaka University, 1-6 Yamadaoka, Suita, Osaka 565-0871, Japan, [2]Laboratory of Biopharmaceutical Research, National Institute of Biomedical Innovation, 7-6-8, Saito-Asagi, Ibaraki, Osaka 567-0085, Japan, [3]The Center for Advanced Medical Engineering and Informatics, Osaka University, 1-6, Yamadaoka, Suita, Osaka 565-0871, Japan, [4]Department of Developmental Medicine, Osaka Medical Center and Research Institute for Maternal and Child Health, 840 Murodo-cho, Izumi, Osaka 594-1101, Japan, [5]Bioresources Research, Laboratory of Common Apparatus, National Institute of Biomedical Innovation, 7-6-8, Saito-Asagi, Ibaraki, Osaka 567-0085, Japan, [6]Vitamin C60 BioResearch Corporation, 1-3-19, Yaesu, Chuo-ku, Tokyo 103-0028, Japan, [7]Mitsubishi Corporation, 2-6-1, Marunouchi, Chiyoda-ku, Tokyo 100-8086, Japan, [8]Graduate School of Pharmaceutical Sciences, Kobe-Gakuin University, 1-1-3, Minatojima, Chuo-ku, Kobe, Hyogo 650-8586, Japan, [9]Department of Biomedical Innovation, Graduate School of Pharmaceutical Sciences, Osaka University, 7-6-8 Saito-asagi, Ibaraki, Osaka 567-0085, Japan, [10]Department of Obstetrics and Gynecology, University of Toyama, 2630, Sugitani, Toyama 930-0194, Japan; †These authors contributed equally to this work.
*e-mail: yasuo@phs.osaka-u.ac.jp; ytsutsumi@phs.osaka-u.ac.jp

potentials of –53, –62, –67, –23 and –13 mV, respectively (see Supplementary Fig S2 for the physicochemical properties of all the materials). The size distribution spectrum of each silica particle showed a single peak (Supplementary Fig. S1m), and the hydrodynamic diameter corresponded almost precisely to the primary particle size for each sample (Supplementary Figs S1m and S2), indicating that the silica particles used in this study were well-dispersed in solution.

We examined the relationship between particle size and biodistribution in the placenta by whole-body imaging analysis after intravenous injection (through the tail vein) of fluorescent DY-676-labelled nSP70, nSP300 or mSP1000 into pregnant mice at gestational day 16 (GD16). At 24 h post-injection, intense fluorescence was observed in the liver of all mice receiving the differently sized nanoparticles (Fig. 1a), suggesting that the accumulation of nanoparticles in the liver is independent of size. Fluorescence was seen in the placenta of mice treated with nSP70, but not in mice treated with nSP300 or mSP1000 (Fig. 1a). We confirmed that ~5% of fluorescent DY-676 dissociated from the silica particles after *in vitro* incubation in phosphate buffered saline (PBS) for 24 h at 37 °C (Supplementary Fig. S1n), and no fluorescence was detected in the placenta of mice treated with fluorescent DY-676 only (data not shown), indicating that the fluorescence observed in the mice was caused by silica particle accumulation in the tissues.

TEM analysis revealed that nSP70 (nanosized spherical black objects in Fig. 1b–g) were found in placental trophoblasts (Fig. 1b,c), fetal liver (Fig. 1d,e) and fetal brain (Fig. 1f,g). No particles were seen in the placenta, fetal liver or fetal brain of mice treated with nSP300 or mSP1000 (data not shown). These results suggest that the biodistribution of silica particles varied according to particle size, and that only the smaller nSP70 nanoparticles accumulated in the placenta and fetus. Similarly, nano-TiO_2 were found in placental trophoblasts (Fig. 1h,i), the fetal liver (Fig. 1j,k) and fetal brain (Fig. 1l,m) after intravenous injection into pregnant mice. We did not evaluate the biodistribution of fullerene C_{60} because of the difficulty in detecting fullerene using TEM.

Recently, several reports have shown that some nanomaterials can penetrate mouse and *ex vivo* human placental tissue[25,28], and it is generally known that high-molecular-weight species (>1,000 Da) do not penetrate the placenta by passive diffusion. Thus, we speculated that nSP70 either directly injured the blood–placenta barrier or was actively transported through it, or both. Furthermore, nSP70 in the fetal circulation would have access to the fetal liver and brain, because the development of the blood–brain barrier in the fetal brain is incomplete[29].

Fetotoxicity of nanoparticles

To determine the fetotoxicity of nSP70, nSP300, mSP1000, nano-TiO_2 and fullerene in pregnant mice, we intravenously injected the particles (100 μl, 0.8 mg per mouse) into pregnant mice on two consecutive days, at GD16 and GD17, and measured the maternal blood biochemistry. None of the silica particles induced any significant changes in the levels of aspartate aminotransferase (AST), alanine aminotransferase (ALT) and blood urea nitrogen (BUN), and all parameters remained within the physiological range, indicating that the particles did not induce maternal liver and kidney damage at the administered doses (Supplementary Fig. S3). Blood pressure and heart rates among all groups of mice that received silica nanoparticles were similar and comparable to control animals receiving PBS (Supplementary Fig. S4). However, there was a significant increase in the number of granulocytes in nSP70-treated pregnant mice compared with control mice receiving PBS (Supplementary Fig. S5).

When compared to control mice, the maternal body weight of nSP70- and nano-TiO_2-treated mice decreased at GD17 and GD18, whereas those treated with nSP300, mSP1000 and fullerenes did not show any changes (Fig. 2a). Mice that received nSP70 and nano-TiO_2 had 20% and 30% lower uterine weights (Fig. 2b,c), respectively, and significantly higher fetal resorption rates than control mice and those that received nSP300, mSP1000 particles or fullerene (Fig. 2d). nSP70- and nano-TiO_2-treated mice also had smaller fetuses (nearly 10% lower than control mice, Fig. 2e,g) and smaller amnion sacs than mice that received nSP300, mSP1000 or fullerene.

In contrast, the weights of placentae were the same among all groups of mice (Fig. 2f,h). When mice were injected with lower concentrations of nSP70 (0.2 and 0.4 mg per mouse), none of the above symptoms was observed; fetal resorption and growth restriction were seen only at the highest dose used (0.8 mg per mouse; Supplementary Fig. S6). These results indicate that only nSP70 at the highest concentration and nano-TiO_2 induced fetal resorption and restricted fetal growth; fullerene did not induce any pregnancy complications. The doses used here are typical of preclinical studies for drug delivery applications of silica particles, intravenously administered at several hundred milligrams per mouse[30]. In contrast, the most common route of nano-TiO_2 exposure to humans is through the skin (for example, through the application of nano-TiO_2-containing cosmetics) and some reports have suggested that nano-TiO_2 particles do not penetrate into living skin[31,32]. Therefore, we believe that nano-TiO_2 may not induce any pregnancy complications following topical application. Furthermore, we have confirmed that the nano-TiO_2 used in this study did not induce cellular toxicity and DNA damage *in vitro* (data not shown).

It is known that the surface properties of nanomaterials can influence biodistribution, inflammatory responses and cellular toxicity[27,33]. We examined the relationship between fetotoxicity and the surface properties of nSP70. The nSP70 was surface-modified with COOH or NH_2 functional groups (nSP70-C or nSP70-N, respectively), and both were confirmed by TEM to be smooth-surfaced spherical particles (Supplementary Fig. S1). The hydrodynamic diameters of the nSP70-C and nSP70-N were 70 and 72 nm, respectively, with zeta potentials of –76 and –29 mV, respectively, indicating that surface modification changed the surface charge of the particles (Supplementary Fig. S2).

As with nSP70, mice that were intravenously injected with DY-676-labelled nSP70-C and nSP70-N showed fluorescence in the placenta (Fig. 1a). TEM analysis revealed that nSP70-C and nSP70-N were found in placental trophoblasts (Fig. 1n,q), fetal liver (Fig. 1o,r) and fetal brain (Fig. 1p,s), indicating that the particles accumulated in the placenta and fetus. The maternal body weights of mice treated with nSP70-C or nSP70-N were the same as those observed for control mice (Fig. 2a). nSP70-C and nSP70-N did not affect the uterine weight (Fig. 2c), fetal weight (Fig. 2e,g) or fetal resorption rate (Fig. 2b,d). These results suggest that modifying the surface of nSP70 can prevent resorption and fetal growth restriction induced by nSP70.

Placental dysfunction in nSP70-treated mice

Normal placental development is required for embryonic growth, and placental dysfunction has been associated with miscarriage and fetal growth restriction[34,35]. The mature murine placenta consists of four layers: maternal decidua, trophoblast giant cell, spongiotrophoblast and labyrinth[34,35] (Fig. 3a). Maternal spiral arteries converge into canals between the trophoblast giant cells, and these canals pass through the spongiotrophoblast and labyrinth layers[34,35]. The exchange of respiratory gases, nutrients and waste takes place in the labyrinth layer between the fetal blood vessels and maternal blood sinuses[34,35].

To clarify the relationship between particle size, fetotoxicity and placental dysfunction, we examined the pathological histology of the placenta in nSP-treated mice using haematoxylin and eosin (H&E) staining (Fig. 3b–e). The placenta of mice treated with nSP70 showed variable structural abnormalities, whereas those treated

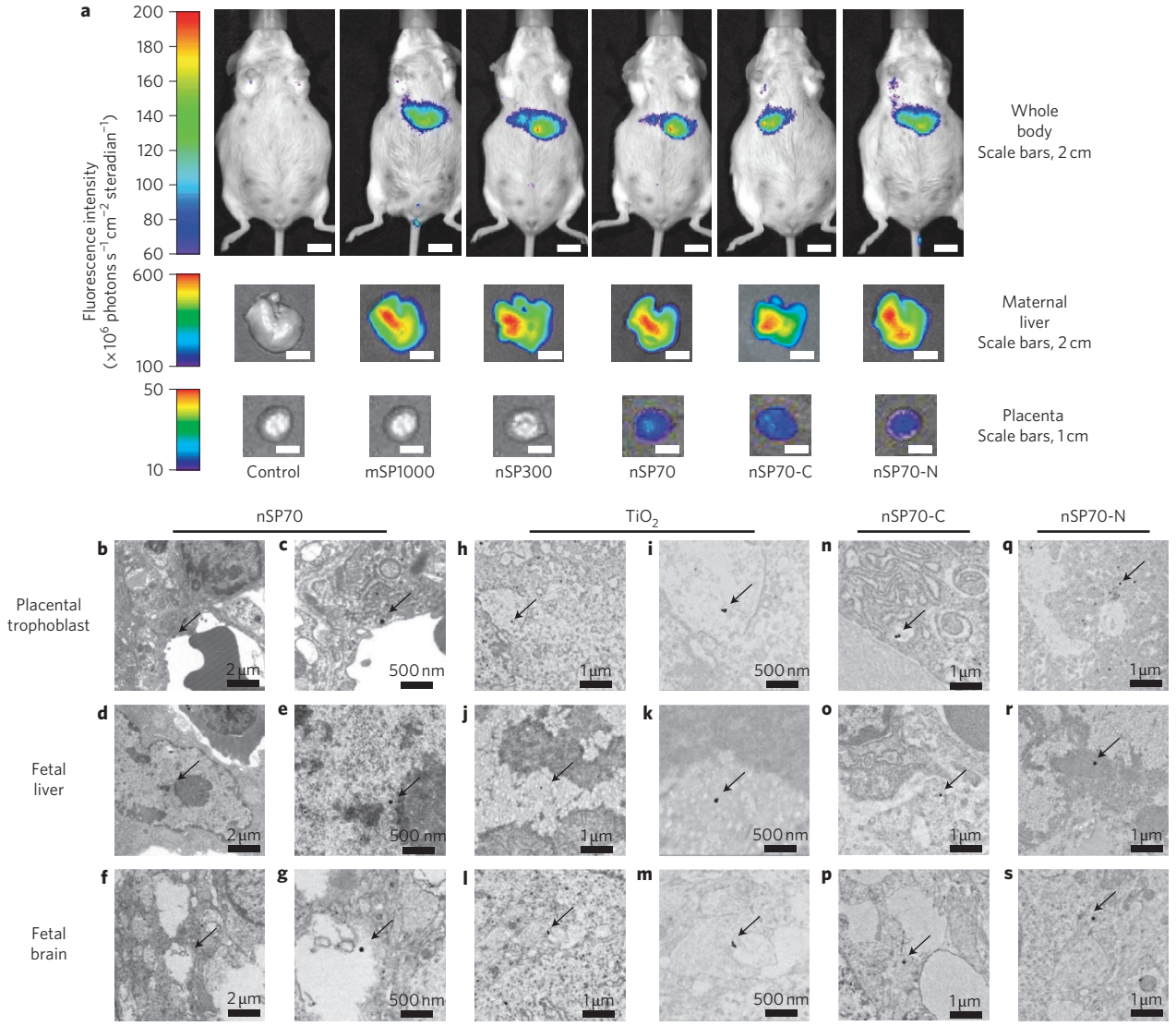

Figure 1 | Biodistribution of nanoparticles in pregnant mice. a, *In vivo* fluorescence images. Pregnant mice at GD16 were treated with 0.8 mg DY-676-labelled silica particles per mouse (nSP70, nSP300, mSP1000, nSP70-C or nSP70-N) or PBS (control), intravenously, through the tail vein. After 24 h, optical images of the whole body, maternal liver and placenta were acquired with a Xenogen IVIS 200 imaging system. **b**–**s**, TEM images of placentae and fetuses at GD18. Pregnant mice were treated intravenously with 0.8 mg per mouse of nSP70, nano-TiO_2, nSP70-C or nSP70-N on two consecutive days (GD16 and GD17). Arrows indicate nanoparticles. These particles were present in placental trophoblast cells (**b**,**c**,**h**,**i**,**n**,**q**), fetal liver cells (**d**,**e**,**j**,**k**,**o**,**r**) and fetal brain cells (**f**,**g**,**l**,**m**,**p**,**s**).

with nSP300 and mSP1000 did not show any significant abnormalities when compared to control mice (Fig 3b,d). Spiral artery canals failed to form (Fig. 3b,d) and blood flow was reduced in the fetal vascular sinuses of nSP70-treated mice (Fig. 3c,e). To further elucidate the influence of nanoparticles on placental dysfunction, we are examining the pathological histology of the placenta in nano-TiO_2-treated mice at present.

The areas including the placental major layers (the spongiotrophoblast and labyrinth) in nSP70-treated and control mice were examined by periodic acid–Schiff (PAS) staining (Fig. 3f–i). The total areas of placentae from each nSP70-treated mouse were not significantly different from those of control mice (Fig. 4a). The area of the spongiotrophoblast layer (Fig. 4b) and the ratio of the spongiotrophoblast layer area to the total placental area (Fig. 4c) in nSP70-treated mice were almost 50% smaller than those observed in control mice. The percentage of nuclei positively stained by terminal transferase-mediated dUTP nick end-labelling (TUNEL) was significantly higher within the spongiotrophoblast layer of nSP70-treated mice than within that of control mice, indicating that nSP70 induced apoptotic cell death of spongiotrophoblasts (Fig. 3j,k; Fig. 4d). The surrounding lengths of the villi in the labyrinth layer of nSP70-treated mice were significantly decreased compared to those of control mice (Fig. 3l,m; Fig. 4f), whereas the ratio of the labyrinth layer area to the total placental area in nSP70-treated mice was not significantly different from that of control mice (Fig. 4e). These results suggest that nSP70-induced pregnancy complications were probably caused by placental cellular damage, which might affect maternal–fetal exchange.

Normal placental development requires the coordinated expression of vascular endothelial growth factor (VEGF) and its receptor, fms-like tyrosine kinase-1 (Flt-1)[36]. Soluble Flt-1 (sFlt-1) is expressed by placental cells including spongiotrophoblasts, and is a potent anti-angiogenic molecule that regulates the generation of placental vasculature during pregnancy by sequestering circulating VEGF and regulating the action of VEGF[37]. The plasma level of sFlt-1 in nSP70- and nano-TiO_2-treated mice was significantly

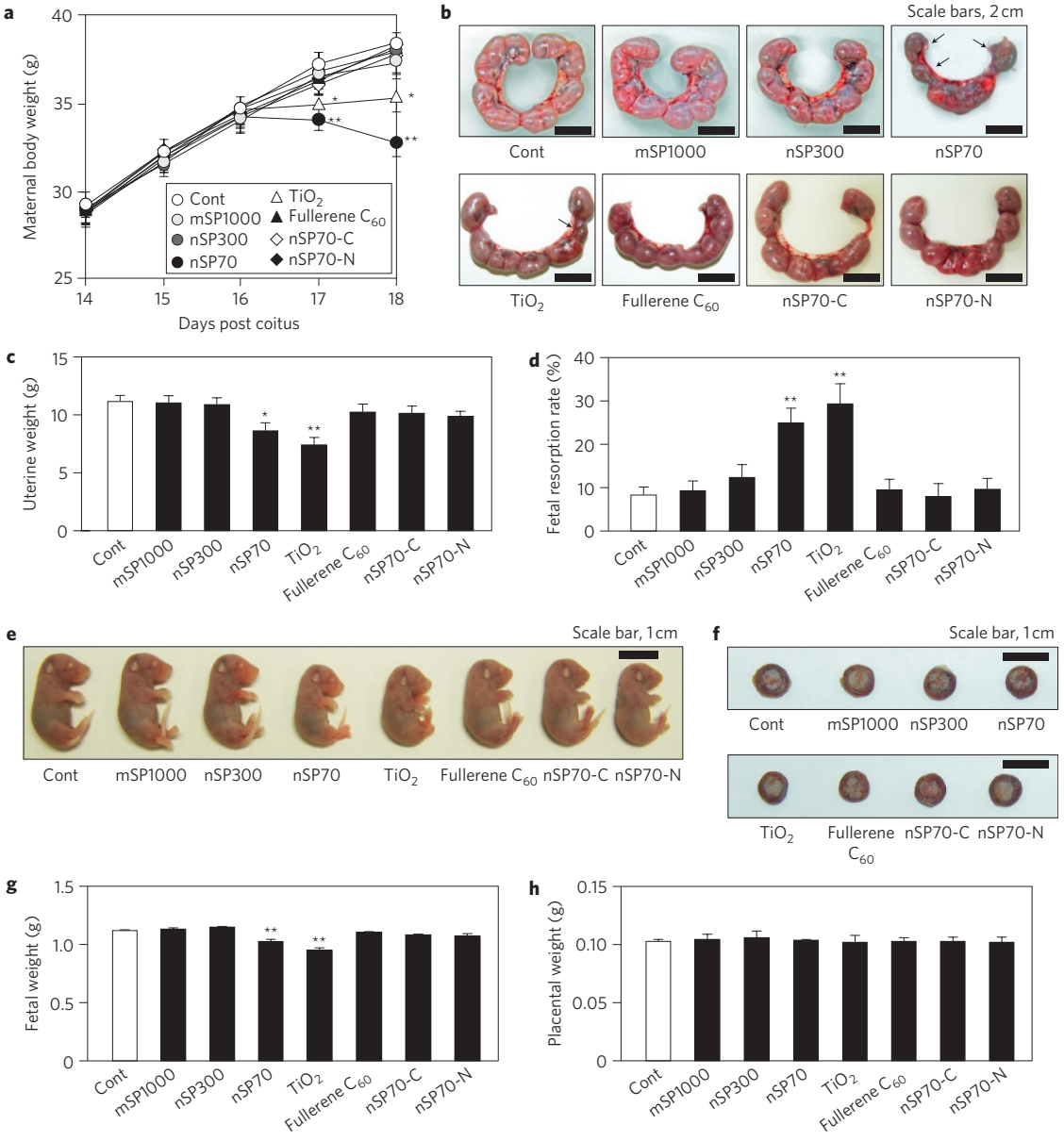

Figure 2 | Pregnancy complications in nSP70- or nano-TiO_2-treated mice. Pregnant mice were treated intravenously with 0.8 mg per mouse of nSP70, nSP300, mSP1000, nano-TiO_2, fullerene C_{60}, nSP70-C, nSP70-N or PBS (control) on two consecutive days (GD16 and GD17). **a**, Changes in maternal body weight. Maternal body weights were evaluated daily ($n = 11$–24). Statistically significant difference from control mice, $^*P < 0.05$ and $^{**}P < 0.01$ by ANOVA. **b**–**h**, Pregnancy complications. Uteri from mice were excised at GD18 (**b**). Uterine weights (**c**) and fetal resorption rates (**d**) were evaluated ($n = 11$–24). Fetuses (**e**) and placentae (**f**) were excised from uteri. Fetal weights (**g**) and placental weights (**h**) were evaluated ($n = 37$–212). All data represent means ± s.e.m ($^*P < 0.05$, $^{**}P < 0.01$ versus value for control mice by ANOVA).

lower than in control mice and those receiving nSP300, mSP1000, fullerene, nSP70-C and nSP70-N (Supplementary Fig. S7a–d), indicating that nSP70 induced not only structural abnormalities, but also functional abnormalities, in the mouse placenta.

The anticoagulation agent heparin is often administered to prevent miscarriage and IUGR[38]. Mice treated with a combination of nSP70 and heparin had slightly increased maternal body weights and decreased fetal resorption rates compared to mice that were not treated with heparin (Fig. 5a,c). Heparin treatment prevented decreases in uterine and fetal weight in nSP70-treated mice (Fig. 5b,d). Mice treated with a combination of nSP70 and heparin had similar levels of sFlt-1 to control mice (Supplementary Fig. S7e). These results suggest that the mechanism for nSP70-induced pregnancy complications might involve coagulation. However, it has recently been shown that heparin acts in many ways other than as an anticoagulant[39–42]. The anti-complement activation effect of heparin has been suggested to be important in mitigating pregnancy complications[40]. Complement activation induces neutrophil activation and this may lead to placental dysfunction, miscarriage, fetal growth restriction or pre-eclampsia[43,44]. Here, we have shown that the number of granulocytes in nSP70-treated mice is significantly higher than in control mice (Supplementary Fig. S5), indicating that nSP70 might have induced complement activation, which may have subsequently activated neutrophils and systemic inflammation.

Some reports have shown that heparin may also act as a placental growth factor, because heparin is known to inhibit placental apoptosis, stimulate placental proliferation and enhance the effect of several growth factors[39,41,42]. Moreover, oxidative stress in the placenta is known to cause placental dysfunction and to induce pregnancy

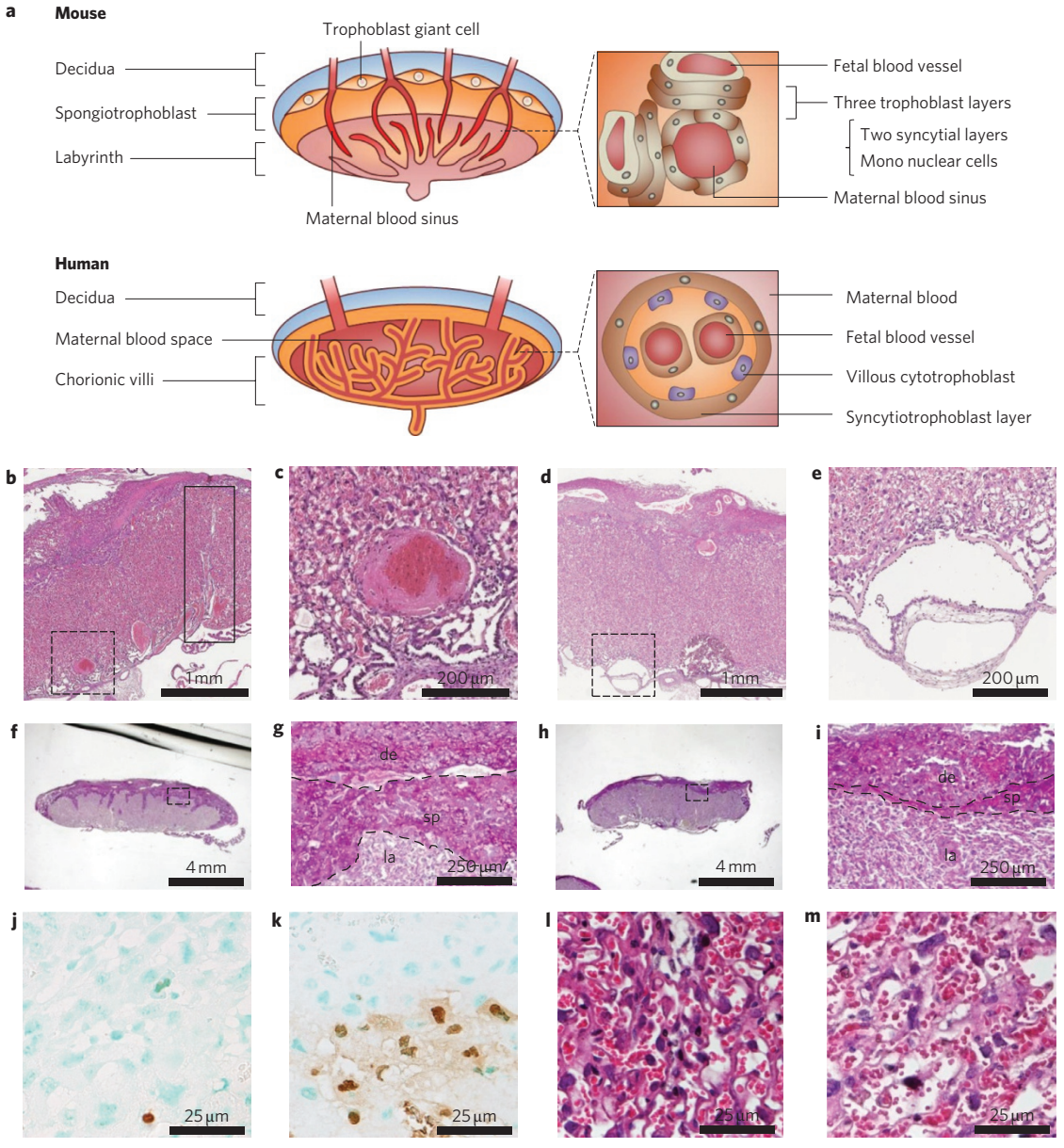

Figure 3 | Pathological examination of placenta. a, Schematic showing the differences between human and mouse placentae. **b**–**m**, Histological examination. Pregnant mice were treated intravenously with 0.8 mg per mouse of nSP70 or PBS (control) on two consecutive days (GD16 and GD17). At GD18, sections of placentae from PBS- (**b**,**c**,**f**,**g**) or nSP70-treated mice (**d**,**e**,**h**,**i**) were stained with H&E (**b**–**e**) or PAS (**f**–**i**). The solid box in **b** indicates the presence of spiral arteries and canals. Panels **c**, **e**, **g**, and **i** are enlarged images of the areas within the dashed boxes in **b**, **d**, **f** and **h**, respectively. In **g** and **i**, dashed lines delineate the decidua (de), spongiotrophoblast layer (sp) and labyrinth layer (la). Spongiotrophoblast layers of PBS- (**j**) or nSP70-treated mice (**k**) were stained with TUNEL. Labyrinth layers of PBS- (**l**) or nSP70-treated mice (**m**) were stained with H&E.

complications[45]. Nanomaterials have been reported to cause oxidative stress, which in turn induces cell apoptosis and inflammation[22,46,47]. Therefore, the pregnancy complications observed here might have been caused by oxidative stress induced by nSP70.

We have observed that the induction of oxidative stress in cells and the activation of the coagulation pathway in mice treated with nSP70-C and nSP70-N were lower than those observed in cells and mice treated with nSP70 (unpublished data). Therefore, we speculate that the lower activation of coagulation, complement and oxidative stress in the placenta of mice treated with nSP70-C and nSP70-N might have prevented pregnancy complications in those mice. It has recently been shown that nanomaterials become coated with serum proteins and induce different cellular responses by binding to proteins[48]. In addition, different surface characteristics, such as surface charge, are known to influence the binding affinities of proteins to nanomaterials[48]. Therefore, the differences in protein binding among nSP70, nSP70-C and nSP70-N might have given rise to differences in the fetotoxicity of the nanomaterials.

It should be noted that there are differences between mouse and human placentae, such as the greater role of yolk sac placentation in the mouse and the anatomy in the labyrinth[49,50] (Fig. 3a). The yolk sac plays a significant role in material transport from mother to fetus in mice, especially before the placental circulation is established[49]. Therefore, the accumulation of nSP70 in the yolk sac should be investigated to understand the accumulation mechanism of nanoparticles in fetuses. In the mouse placenta, three trophoblast layers embrace the fetal vasculature in the labyrinth layer, whereas in the human term placenta, a single syncytial layer with an underlying trophoblast stem cell layer is present in the villi[49,50]. As these anatomical and structural differences might affect nanoparticle

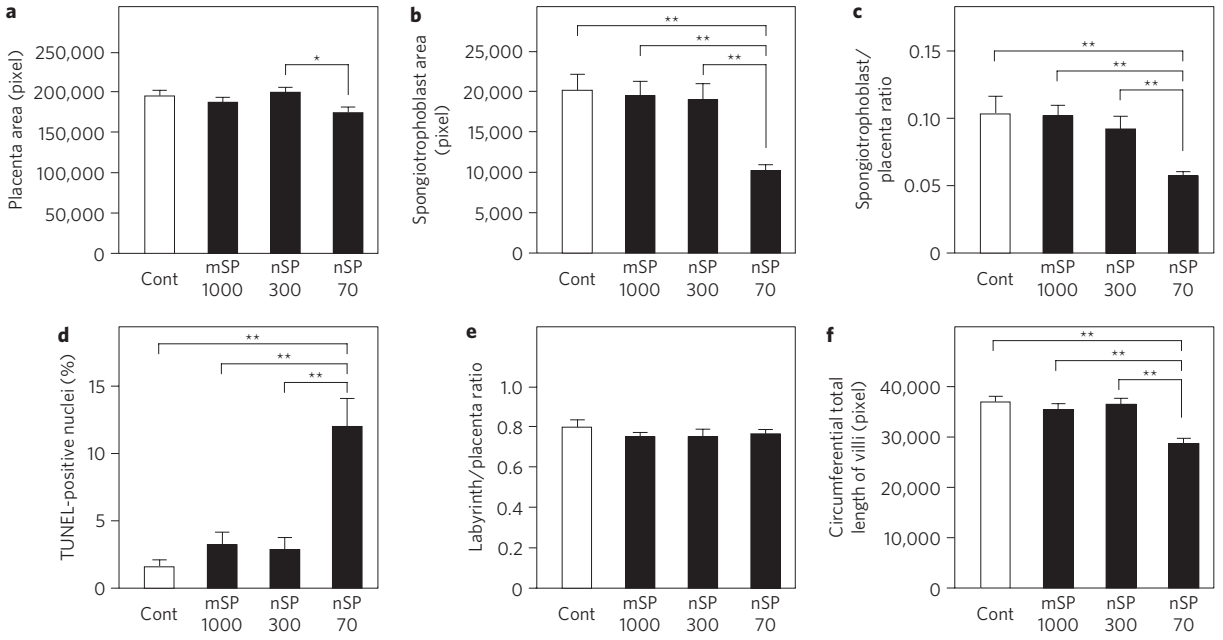

Figure 4 | Dysfunction of placentae. Pregnant mice were treated intravenously with 0.8 mg per mouse of nSP70, nSP300, mSP1000 or PBS (control) on two consecutive days (GD16 and GD17). **a**–**e**, At GD18, the area of the placenta (**a**) and the spongiotrophoblast layer (**b**) and the ratios of the spongiotrophoblast layer area to the total placental area (**c**) and of the labyrinth layer area to the total placental area (**e**) were assessed by examining the PAS-stained sections in Fig. 3f–i and were analysed quantitatively. The apoptotic index (**d**) was assessed by examining the TUNEL-stained sections in Fig. 3j,k and was quantitatively analysed. The surrounding length of the villi (**f**) in the labyrinth layers was assessed by examining the H&E-stained sections in Fig. 3l,m and was quantitatively analysed. All data represent means ± s.e.m. ($n = 11$–20; $^{*}P < 0.05$ and $^{**}P < 0.01$ by ANOVA).

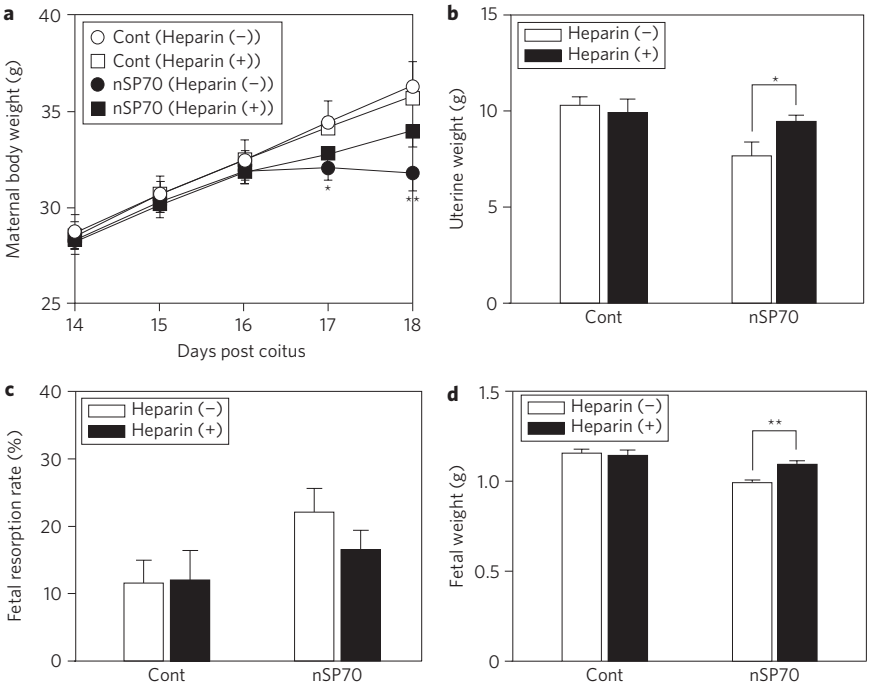

Figure 5 | Prevention of nSP70-induced pregnancy complications with heparin. Pregnant mice were treated intravenously with 0.8 mg per mouse of nSP70 or PBS (control) through the tail vein with or without heparin on two consecutive days (GD16 and GD17). **a**, Changes in maternal body weights. Maternal body weights were evaluated daily ($n = 10$–15). Statistically significant difference from control mice, $^{*}P < 0.05$ and $^{**}P < 0.01$ by ANOVA. **b**–**d**, Analysis of pregnancy complications in nSP70-treated mice with or without heparin treatment. At GD18, uterine weights (**b**), fetal resorption rates (**c**) and fetal weights (**d**) were evaluated (**b**,**c**, $n = 10$–15; **d**, $n = 55$–89). All data represent means ± s.e.m., $^{*}P < 0.05$ and $^{**}P < 0.01$ by Student's *t*-tests.

uptake and distribution, we cannot extrapolate our data about the placental distribution of nanoparticles, or placental dysfunction induced by nanoparticles, to humans. Additional studies that examine the penetration efficiency of nanoparticles into the human placenta (using *ex vivo* human placental tissue) are needed, as are studies that focus on the relationship between pregnancy complications and the amount of nanoparticles in the human placenta.

Conclusion

Of the materials studied here, nSP70 and nano-TiO_2 induced fetal resorption and restricted the growth of fetuses in pregnant mice, whereas fullerene C_{60} did not induce these complications. nSP70 and nano-TiO_2 were observed in the placenta, fetal liver and fetal brain, and nSP70 induced complications only at the highest concentration (0.8 mg per mouse) administered. The detrimental effects seen in nSP70-treated mice were linked to structural and functional changes in the placenta. Modification of the surface of nSP70 with carboxyl or amine groups abrogated the negative effects, suggesting the importance of surface charge. Although the nSP70 and nano-TiO_2 were mainly designed for experimental and industrial use, and not for cosmetics or food, we suggest that the potential fetotoxicity of these and other nanomaterials should be investigated more carefully.

Methods

Particles. nSP70, nSP300, mSP1000, nSP70-C and nSP70-N, as well as nSP70, nSP300 and mSP1000 labelled with DY-676 (excitation and emission wavelengths of 674 and 699 nm, respectively), were purchased from Micromod Partikeltechnologie. Rutile-type TiO_2 particles with a diameter of 35 nm (designated nano-TiO_2, Tayca Corporation) were also used. Polyvinylpyrrolidone (PVP)-wrapped fullerene C_{60} was provided by Vitamin C60 BioResearch Corporation. The nanoparticles were used after 5 min of sonication (280 W output (Ultrasonic Cleaner, AS One) and 1 min of vortexing.

Mice. Pregnant BALB/c mice (8–10 weeks) were purchased from Japan SLC. The experimental protocols conformed to the ethical guidelines of Osaka University and the National Institute of Biomedical Innovation, Japan.

***In vivo* imaging.** *In vivo* fluorescence imaging was performed with an IVIS 200 small-animal imaging system (Xenogen). At GD16, pregnant BALB/c mice were injected with 100 μl (0.8 mg per mouse) DY-676-labelled nSP70, nSP300, mSP1000, nSP70-C, nSP70-N or PBS (control), intravenously through the tail vein. At 24 h post-injection, the mice were anaesthetized, and images were obtained with a cy5.5 filter set (excitation/emission, 615–665 nm/695–770 nm). Imaging parameters were selected and implemented with Living Image 2.5 software (Xenogen).

TEM analysis. Pregnant BALB/c mice were treated with 100 μl (0.8 mg per mouse) of nSP70, nSP300, mSP1000, nSP70-C, nSP70-N or nano-TiO_2, intravenously through the tail vein, on two consecutive days (GD16 and GD17). At GD18, mice were killed after being anaesthetized, and the placenta, fetal liver and fetal brain were fixed in 2.5% glutaraldehyde for 2 h. Small pieces of tissue collected from these samples were washed with phosphate buffer, postfixed in sodium cacodylate-buffered 1.5% osmium tetroxide for 60 min at 4 °C, dehydrated using a series of ethanol concentrations, and embedded in Epon resin. The samples were examined under a Hitachi electron microscope (H-7650; Hitachi).

Fetotoxicity. Pregnant BALB/c mice were treated with 100 μl of nSP70 (0.2 mg, 0.4 mg or 0.8 mg per mouse), nSP300 (0.8 mg per mouse), mSP1000 (0.8 mg per mouse), nSP70-C (0.8 mg per mouse), nSP70-N (0.8 mg per mouse), nano-TiO_2 (0.8 mg per mouse), fullerene C_{60} (0.8 mg per mouse) or PBS (control), intravenously through the tail vein, on two consecutive days (GD16 and GD17). All mice were killed after being anaesthetized at GD18. Blood samples were collected in tubes containing 5 IU ml^{-1} heparin sodium, and plasma was harvested. The rate of fetal resorption was calculated (number of resorptions/total number of formed fetuses and resorptions). The fetuses and placentae of each mouse were excised and weighed, and the weight of the uterus calculated as the sum of the placental and fetal weights. To study the effects of heparin in nSP70-treated mice, pregnant BALB/c mice were treated with 100 μl (0.8 mg per mouse) nSP70 or PBS (control) intravenously through the tail vein on two consecutive days (GD16 and GD17). The same mice were treated with heparin (Sigma-Aldrich, 10 U) intraperitoneally on two consecutive days (GD16 and GD17), twice a day, 3 h before nSP70 treatment and 3 h after nSP70 treatment.

Histological examination. After fixing placentae in 10% formalin neutral buffer solution overnight, tissues were washed in PBS, dehydrated in a graded series of ethanol and xylene solutions, and embedded in paraffin. Sections (2 μm) were cut with a microtome. Sections were deparaffinized, rehydrated in a graded series of ethanols, and stained with H&E or PAS. Stained sections were dehydrated in a series of ethanols and mounted using permount. Representative histological images were recorded with a charge-coupled device (CCD) digital camera fixed to a microscope. The areas of the placenta, spongiotrophoblast layer and labyrinth layer were assessed by examining light microscopy images (Olympus) of the PAS-stained sections and were quantitatively analysed with Image J Imaging System Software Version 1.3 (National Institutes of Health). The circumferential total length of villi was assessed by examining light microscopy images of the H&E-stained sections and quantitatively analysed with Image J Imaging System Software Version 1.3. The presence of apoptotic cells in placental sections was analysed by TUNEL assay (Millipore). The tissue was counterstained with methyl green. Photographs of TUNEL (brown) and methyl green (light blue) staining were captured at three randomly selected fields in the spongiotrophoblast layer. TUNEL-positive nuclei (apoptotic nuclei) and methyl green-stained nuclei (total nuclei) were counted in the spongiotrophoblast layer. The apoptotic index in each section was calculated as the percentage of spongiotrophoblast nuclei stained TUNEL-positive divided by the total number of methyl green-stained nuclei found within the spongiotrophoblast layer.

Statistical analysis. All results are presented as means ± standard error of the mean (s.e.m.). Statistical significance in the differences was evaluated by Student's *t*-tests or Tukey's method after analysis of variance (ANOVA).

Received 23 September 2010; accepted 28 February 2011; published online 3 April 2011

References

1. Konstantatos, G. & Sargent, E. H. Nanostructured materials for photon detection. *Nature Nanotech.* **5,** 391–400 (2010).
2. Augustin, M. A. & Sanguansri, P. Nanostructured materials in the food industry. *Adv. Food. Nutr. Res.* **58,** 183–213 (2009).
3. Bowman, D. M., van Calster, G. & Friedrichs, S. Nanomaterials and regulation of cosmetics. *Nature Nanotech.* **5,** 92 (2010).
4. Petros, R. A. & DeSimone, J. M. Strategies in the design of nanoparticles for therapeutic applications. *Nature Rev. Drug Discov.* **9,** 615–627 (2010).
5. Martin, K. R. The chemistry of silica and its potential health benefits. *J. Nutr. Health Aging.* **11,** 94–97 (2007).
6. Knopp, D., Tang, D. & Niessner, R. Review: bioanalytical applications of biomolecule-functionalized nanometer-sized doped silica particles. *Anal. Chim. Acta.* **647,** 14–30 (2009).
7. Kagan, V. E., Bayir, H. & Shvedova, A. A. Nanomedicine and nanotoxicology: two sides of the same coin. *Nanomedicine* **1,** 313–316 (2005).
8. Nel, A., Xia, T., Madler, L. & Li, N. Toxic potential of materials at the nanolevel. *Science* **311,** 622–627 (2006).
9. Fadeel, B. & Garcia-Bennett, A. E. Better safe than sorry: understanding the toxicological properties of inorganic nanoparticles manufactured for biomedical applications. *Adv. Drug. Deliv. Rev.* **62,** 362–374 (2010).
10. Poland, C. A. *et al.* Carbon nanotubes introduced into the abdominal cavity of mice show asbestos-like pathogenicity in a pilot study. *Nature Nanotech.* **3,** 423–428 (2008).
11. Donaldson, K., Murphy, F. A., Duffin, R. & Poland, C. A. Asbestos, carbon nanotubes and the pleural mesothelium: a review of the hypothesis regarding the role of long fibre retention in the parietal pleura, inflammation and mesothelioma. *Part. Fibre Toxicol.* **7,** 5 (2010).
12. Nabeshi, H. *et al.* Systemic distribution, nuclear entry and cytotoxicity of amorphous nanosilica following topical application. *Biomaterials* **32,** 2713–2724 (2011).
13. Nabeshi, H. *et al.* Amorphous nanosilica induce endocytosis-dependent ROS generation and DNA damage in human keratinocytes. *Part. Fibre Toxicol.* **8,** 1 (2011).
14. Koren, G., Pastuszak, A. & Ito, S. Drugs in pregnancy. *N. Engl. J. Med.* **338,** 1128–1137 (1998).
15. Tardiff, R. G., Carson, M. L. & Ginevan, M. E. Updated weight of evidence for an association between adverse reproductive and developmental effects and exposure to disinfection by-products. *Regul. Toxicol. Pharmacol.* **45,** 185–205 (2006).
16. Wigle, D. T. *et al.* Epidemiologic evidence of relationships between reproductive and child health outcomes and environmental chemical contaminants. *J. Toxicol. Environ. Health. B. Crit. Rev.* **11,** 373–517 (2008).
17. Mills, J. L. *et al.* Incidence of spontaneous abortion among normal women and insulin-dependent diabetic women whose pregnancies were identified within 21 days of conception. *N. Engl. J. Med.* **319,** 1617–1623 (1988).
18. Cetin, I. & Alvino, G. Intrauterine growth restriction: implications for placental metabolism and transport. A review. *Placenta* **30(Suppl. A),** S77–S82 (2009).
19. Godfrey, K. M. & Barker, D. J. Fetal nutrition and adult disease. *Am. J. Clin. Nutr.* **71,** 1344S–1352S (2000).
20. Barker, D. J. Adult consequences of fetal growth restriction. *Clin. Obstet. Gynecol.* **49,** 270–283 (2006).
21. Takeda, K. *et al.* Nanoparticles transferred from pregnant mice to their offspring can damage the genital and cranial nerve systems. *J. Health Sci.* **55,** 95–102 (2009).
22. Shimizu, M. *et al.* Maternal exposure to nanoparticulate titanium dioxide during the prenatal period alters gene expression related to brain development in the mouse. *Part. Fibre Toxicol.* **6,** 20 (2009).
23. Tian, F. *et al.* Surface modification and size dependence in particle translocation during early embryonic development. *Inhal. Toxicol.* **21(Suppl. 1),** 92–96 (2009).
24. Saunders, M. Transplacental transport of nanomaterials. *Wiley Interdiscip. Rev. Nanomed. Nanobiotechnol.* **1,** 671–684 (2009).

25. Chu, M. *et al.* Transfer of quantum dots from pregnant mice to pups across the placental barrier. *Small* **6,** 670–678 (2010).
26. Hougaard, K. S. *et al.* Effects of prenatal exposure to surface-coated nanosized titanium dioxide (UV-Titan). A study in mice. *Part. Fibre Toxicol.* **7,** 16 (2010).
27. He, X. *et al. In vivo* study of biodistribution and urinary excretion of surface-modified silica nanoparticles. *Anal. Chem.* **80,** 9597–9603 (2008).
28. Wick, P. *et al.* Barrier capacity of human placenta for nanosized materials. *Environ. Health Perspect.* **118,** 432–436 (2010).
29. Watson, R. E., Desesso, J. M., Hurtt, M. E. & Cappon, G. D. Postnatal growth and morphological development of the brain: a species comparison. *Birth Defects Res. B. Dev. Reprod. Toxicol.* **77,** 471–484 (2006).
30. Li, L. *et al. In vivo* delivery of silica nanorattle encapsulated docetaxel for liver cancer therapy with low toxicity and high efficacy. *ACS Nano.* **4,** 6874–6882 (2010).
31. Filipe, P. *et al.* Stratum corneum is an effective barrier to TiO_2 and ZnO nanoparticle percutaneous absorption. *Skin Pharmacol. Physiol.* **22,** 266–275 (2009).
32. Sadrieh, N. *et al.* Lack of significant dermal penetration of titanium dioxide from sunscreen formulations containing nano- and submicron-size TiO_2 particles. *Toxicol. Sci.* **115,** 156–166 (2010).
33. Albrecht, C. *et al.* Inflammatory time course after quartz instillation: role of tumor necrosis factor-alpha and particle surface. *Am. J. Respir. Cell. Mol. Biol.* **31,** 292–301 (2004).
34. Kibschull, M., Gellhaus, A. & Winterhager, E. Analogous and unique functions of connexins in mouse and human placental development. *Placenta* **29,** 848–854 (2008).
35. Gasperowicz, M. & Otto, F. The notch signalling pathway in the development of the mouse placenta. *Placenta* **29,** 651–659 (2008).
36. Lam, C., Lim, K. H. & Karumanchi, S. A. Circulating angiogenic factors in the pathogenesis and prediction of preeclampsia. *Hypertension* **46,** 1077–1085 (2005).
37. Hirashima, M., Lu, Y., Byers, L. & Rossant, J. Trophoblast expression of fms-like tyrosine kinase 1 is not required for the establishment of the maternal–fetal interface in the mouse placenta. *Proc. Natl Acad. Sci. USA* **100,** 15637–15642 (2003).
38. Derksen, R. H., Khamashta, M. A. & Branch, D. W. Management of the obstetric antiphospholipid syndrome. *Arthritis Rheum.* **50,** 1028–1039 (2004).
39. Li, Y., Wang, H. Y. & Cho, C. H. Association of heparin with basic fibroblast growth factor, epidermal growth factor, and constitutive nitric oxide synthase on healing of gastric ulcer in rats. *J. Pharmacol. Exp. Ther.* **290,** 789–796 (1999).
40. Girardi, G., Redecha, P. & Salmon, J. E. Heparin prevents antiphospholipid antibody-induced fetal loss by inhibiting complement activation. *Nature Med.* **10,** 1222–1226 (2004).
41. Hills, F. A. *et al.* Heparin prevents programmed cell death in human trophoblast. *Mol. Hum. Reprod.* **12,** 237–243 (2006).
42. Hossain, N., Schatz, F. & Paidas, M. J. Heparin and maternal fetal interface: why should it work to prevent pregnancy complications? *Thromb. Res.* **124,** 653–655 (2009).
43. Girardi, G., Yarilin, D., Thurman, J. M., Holers, V. M. & Salmon, J. E. Complement activation induces dysregulation of angiogenic factors and causes fetal rejection and growth restriction. *J. Exp. Med.* **203,** 2165–2175 (2006).
44. Redecha, P., van Rooijen, N., Torry, D. & Girardi, G. Pravastatin prevents miscarriages in mice: role of tissue factor in placental and fetal injury. *Blood* **113,** 4101–4109 (2009).
45. Myatt, L. & Cui, X. Oxidative stress in the placenta. *Histochem. Cell. Biol.* **122,** 369–382 (2004).
46. Hussain, S. *et al.* Oxidative stress and proinflammatory effects of carbon black and titanium dioxide nanoparticles: role of particle surface area and internalized amount. *Toxicology* **260,** 142–149 (2009).
47. Liu, X. & Sun, J. Endothelial cells dysfunction induced by silica nanoparticles through oxidative stress via JNK/P53 and NF-κB pathways. *Biomaterials* **31,** 8198–8209 (2010).
48. Lundqvist, M. *et al.* Nanoparticle size and surface properties determine the protein corona with possible implications for biological impacts. *Proc. Natl Acad. Sci. USA* **105,** 14265–14270 (2008).
49. Enders, A. C. & Blankenship, T. N. Comparative placental structure. *Adv. Drug Deliv. Rev.* **38,** 3–15 (1999).
50. Rossant, J. & Cross, J. C. Placental development: lessons from mouse mutants. *Nature Rev. Genet.* **2,** 538–548 (2001).

Acknowledgements

This study was supported in part by Grants-in-Aid for Scientific Research from the Ministry of Education, Culture, Sports, Science and Technology of Japan (MEXT) and from the Japan Society for the Promotion of Science (JSPS) through a Knowledge Cluster Initiative (MEXT). It was also supported by Health Labour Sciences Research Grants from the Ministry of Health, Labour and Welfare of Japan (MHLW), by a Global Environment Research Fund from the Minister of the Environment, and by the Food Safety Commission (Cabinet Office), the Cosmetology Research Foundation, the Smoking Research Foundation and the Takeda Science Foundation.

Author contributions

K.Y. and Y.Y. designed the study. K.Y., K.H., K.M., Y. Morishita, M.N., T. Yoshida, T.O., H.N., K.N., Y.A., H.K., Y. Monobe and T.I. performed the experiments. K.Y. and Y.Y. collected and analysed the data. K.Y. and Y.Y. wrote the manuscript. H.A., K.S., Y.K., T.M., S.T., N.I., I.Y., S.S. and T. Yoshikawa provided technical support and conceptual advice. Y.T. supervised the project. All authors discussed the results and commented on the manuscript.

Additional information

The authors declare no competing financial interests. Supplementary information accompanies this paper at www.nature.com/naturenanotechnology. Reprints and permission information is available online at http://npg.nature.com/reprintsandpermissions/. Correspondence and requests for materials should be addressed to Y.Y. and Y.T.